Heterogeneous & Homogeneous & Bio- & Nano-
CHEMCATCHEM
CATALYSIS

Accepted Article

Title: Multi-Step Organic Transformations over Base-Rhodium/diamine-Bifunctionalized Mesostructured Silica Nanoparticles

Authors: Guohua Liu, Han Liao, Yajie Chou, Yu Wang, Han Zhang, and Tanyu Cheng

To be cited as: *ChemCatChem* 10.1002/cctc.201700436

Link to VoR: http://dx.doi.org/10.1002/cctc.201700436

A Journal of
ChemPubSoc Europe

WILEY-VCH

www.chemcatchem.org

FULL PAPERS

DOI: 10.1002/cctc.200((will be filled in by the editorial staff))

Multi–Step Organic Transformations over Base–Rhodium/diamine–Bifunctionalized Mesostructured Silica Nanoparticles

Hang Liao, Yajie Chou, Yu Wang, Han Zhang, Tanyu Cheng and Guohua Liu*

Dedication ((optional))

Abstract: Assembly of multiple catalytically functionalities within a single mesoporous silica as a catalyst for multi-step enantioselective organic transformation in an environmentally friendly medium is a significant challenge in heterogeneous asymmetric catalysis. Herein, taking advantage of $BF4^-$ anion hydrogen bonding strategy, we anchor conviently a chiral cationic rhodium/diamine complex within base–functionalized mesostructured silica nanoparticles, constructing a bifunctional heterogeneous catalyst. Solid-state carbon spectrum discloses its well-defined chiral rhodium/diamine active species, and its X-ray diffraction, nitrogen adsorption–desorption measurement and electron microscopy reveal its ordered mesostructure. As presented in this study, the combination of bifunctionality in silica nanoparticle enables two kinds of efficiently enantioselective organin transformations with high yields and enantioselectivities, wher asymmetric transfer hydrogenation of α–haloketones followed by a epoxidation process provides various chiral aryloxirane while th amination of α–haloketones with anilines followed by asymmetri transfer hydrogenation produces various β-amino alcohols Furthermore, catalyst can be recovered and recycled for seven time without loss of its catalytic activity, showing an attracting feature fo multi-step organic transformations in a sustainable benign process

Introduction

With extensive applications of mesostructured materials in catalysis, such as mesoporous silica/carbon and metal-organic-frameworks, integration of multiple catalytically functionalities within a single mesoporous material for construction of multifunctional catalysts has attracted great interest in heterogeneous asymmetric catalysis.[1] Main advantages are attributed to two aspects of benefits that derived from the specificity of mesostructured silicas,[2] One is that a suitable mesostructured silica can assemble multifunctionality within its nanochannels, and another benefit is that the assembled multifunctionality can eliminate their cross-interactions over an site-isolation immobilization strategy. These potential advantages in construction of multifunctional heterogeneous catalysts are beneficial to multi-step sequential reactions, making unfeasible sequential reaction in a homogenous condition possibilty. Furthermore, an expected cooperative effect of multifunctionality in a single mesostructured silica can further promote catalyti performance, boosting greatly reactivity and/or selectivity. Despit some explorations made in construction of bifunctional catalyst through site-isolation immobilization for multi-step sequentia reactions,[3] construction of a mesostructured silica-base bifunctional heterogeneous catalyst and application it i asymmetric catalysis, especially in a sequential enantioselectiv organic transformation to enhance reactivity an enantioselectivity, are still rare thereby a significant challenge.

Homogeneous chiral N-sulfonylated diamine-base organometallic complexes,[4] especially their cationic rhodiur complexes, are a kind of highly efficient asymmetric transfe hydrogenation (ATH) catalysts that have been applied extensivel in various ATH of 2–haloketones to chiral 2–haloethanols.[5] As a important synthetic motif, chiral 2–haloethanols and derivative are attracting because they could be converted continuously int various pharmaceutical intermediates in medical chemistry.[Therefore, design of a bifunctional heterogeneous catalyst t explorate the application of chiral 2–haloethanols in a sequentia organic transformation is highly desirable.

Interestingly, recent efforts in a hydrogen bonding of counter ion[7] offer a new opportunity for facile assembly of a bifunctional heterogeneous catalyst. Based on this consideration, together with our recent efforts in construction of bifunctional heterogeneous catalysts,[8] herein, we report the facile construction of a base–rhodium/diamine–bifunctionalized heterogeneous catalyst. It was assembled by bonding cationic rhodium/diamine complex onto the basic DABCO-functionalized (DABCO[9] = 1-(3-(triethoxysilyl)propyl)-1,4-

Prof. Guohua Liu.
Key Laboratory of Resource Chemistry of Ministry of Education, Shanghai Key Laboratory of Rare Earth Functional Materials, Shanghai Normal University
Address: No.100 Guilin Rd.
Fax: (+) (0086)216432280
E-mail: ghliu@shnu.edu.cn

Supporting information for this article is available on the WWW under http://dx.doi.org/10.1002/cctc.200xxxxxx.((Please delete if not appropriate))

10.1002/cctc.201700436

diazabicyclo[2.2.2]octan-1-ium chloride) mesostructured silica nanospheres (MSNs)[10] *via* this hydrogen bonding method. Prominent feature is that the designed MSNs are the short-channels, which are beneficial to mass transfer and overcome the drawback of reaction rate in heterogeneous catalysis, enhanceing greatly the catalytic efficiency. As presented in this study, this cationic rhodium/diamine complex in MSNs as a chiral catalytic promoter performs a haloketone–to–haloethanol transformation whereas the DABCO in MSNs as a base enables haloethanol–to–epoxidation transformation. The study used here not only offers a simple approach to construct bifunctional catalyst and to retain original molecular catalyst but also performs an amination-relay-ATH one-pot enantioselective organic transformation for synthesis of chiral β-amino alcohols in an environmental friendly medium.

Results and Discussion

Synthesis and structural characterization of the heterogeneous catalyst

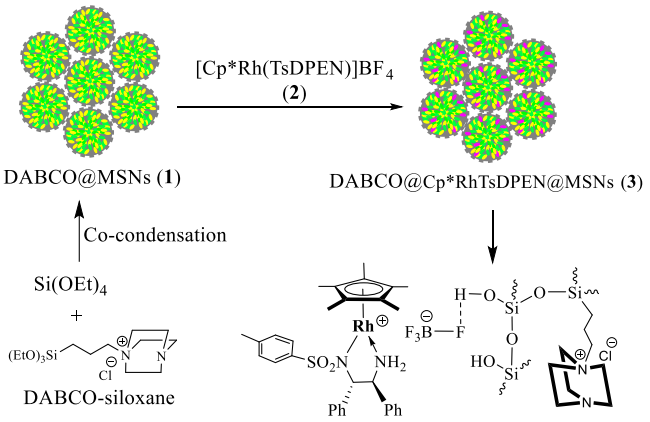

Scheme 1. Preparation of catalysts **3**.

Bifunctional heterogeneous catalyst was prepared by incorporation of chiral ion-pair $(Cp^*RhTsDPEN)^+(BF_4)^-$ within the basic MSNs, abbreviated as DABCO@$(Cp^*RhTsDPEN)^+BF_4^-$@MSNs (**3**) ($Cp^*RhTsDPEN$):[11] Cp* = pentamethyl cyclopentadiene, TsDPEN = N-((*S*,*S*)-2-amino-1,2-diphenylethyl)-4-ethylbenzenesulfonamide). As outlined in Scheme 1, the co-condensation of DABCO-derived siloxane and tetraethoxysilane (TOES) through the use of cetyltrimethylammonium bromide as a structure-directing template led to a basic DABCO@MSNs (**1**) as a white powder. The hydrogen bonding of $(Cp^*RhTsDPEN)^+BF_4^-$ (**2**) within **1** *via* the BF_4^- anion to surface silanols[7] then afforded the crude DABCO@$(Cp^*RhTsDPEN)^+BF_4^-$@MSNs (**3**). Finally, this crude material was subjected to Soxhlet extraction to clearness of its nanochannels and to give its pure heterogeneous catalyst **3** as a light-yellow powder (see SI in Figures S1-S3).

Preservation of the $(Cp^*RhTsDPEN)^+BF_4^-$ molecular structure within its silicate network could be determined by the solid-state NMR spectra (Figure 1). As shown in the ^{13}C CP MAS NMR spectra (Figure 1a), besides the general carbon signals in DABCO moiety and the carbon signals in TsDPEN moiety marked in their spectra, the spectrum of catalyst **3** exhibited the characteristic carbon signals at 96.5 ppm for the aromatic carbon atoms of Cp rings and that at 9.5 ppm for the methyl carbon atoms attached to Cp ring in $CpMe_5$ moiety. These characteristic carbon signals are absent in the spectrum of **1**, demonstrating the successful preservation of the original molecular structure since they were similar to those of its homogeneous $(Cp^*RhTsDPEN)^+BF_4^-$ (**2**).[12] This finding revealed that catalyst **3** had the same well-defined single-site active species as its homogeneous counterpart. Binding cationic rhodium/diamine complex through BF_4^- anion within its MSNs was also confirmed by the solid-state ^{19}F MAS NMR spectrum. As shown in Figure 1b, catalyst **3** produced two groups of F resonances. One groups F resonances are attributed to the free BF_4^- anion at −123.6 ppm,[7a] where the other signals (at −166.0, −144.8, −102.4, and −81.0 ppm) denoted by asterisks were its rotational sidebands calculated by chemical shifts that often appeared in the MAS high-speed rotation process. Another groups wide F resonance between −142 and −156 ppm are assigned to F signals in BF_4 anions interacting with Rh(III) centres of th $(Cp^*RhTsDPEN)^+BF_4^-$ complex *via* the BF_4^- hydrogen bondin proved by its homogeneous liquid-state ^{19}F NMR spectrum (se SI in Fig. S4).[7b-7d]

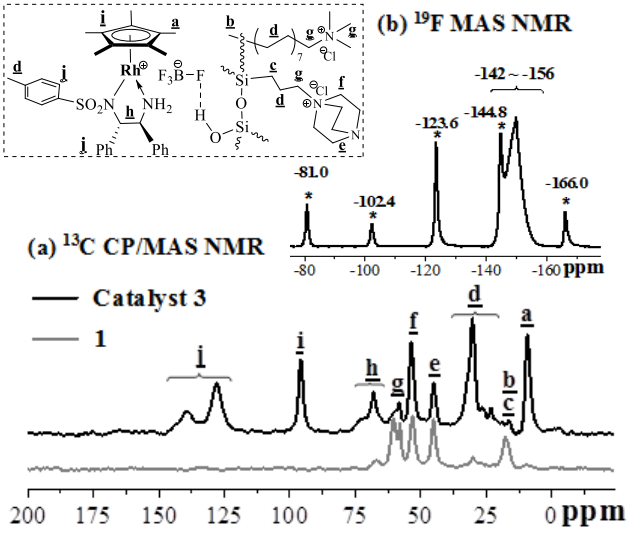

Figure 1. Solid-state CP/MAS NMR spectra of **1** and catalyst **3**.

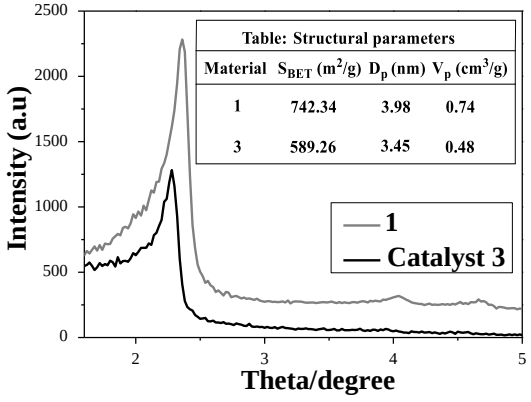

Figure 2. Small-angle powder XRD patterns of **1** and catalyst **3**.

Meanwhile, its X-ray diffraction (XRD), nitrogen adsorption–desorption measurement, transmission electron microscopy

10.1002/cctc.201700436

(TEM), and scanning electron microscopy (SEM) further demonstrated the ordered mesostructure of catalyst **3**. As shown in Figure 2, the small-angle XRD patterns revealed that catalyst **3** had a well-resolved peak at 2θ = 0.8°–1.0°, which was similar to its parent counterpart, indicating the ordered short-channels.[10a] Nitrogen adsorption–desorption isotherms **(**Figure 3) futher demonstrated its mesoporous structure of catalyst **3** due to the presence of typical type IV isotherm with an H_1 hysteresis loop. Their structural parameters were listed in a Table that was an inset in Figure 2, where the decreased mesopore size, surface area, and pore volume of catalyst **3** relative to those of **1** indicated that the coverage of pore surface with the $(Cp^*RhTsDPEN)^+BF_4^-$ complexes led to an increase of the wall thickness. Figure 4 presented the morphologies of catalyst **3.** The SEM images revealed the monodisperse nanoparticules of catalyst **3** with an average size of about 140 nm (Figure 4a), whereas the TEM images further confirmed its ordered mesostructure (Figure 4b).

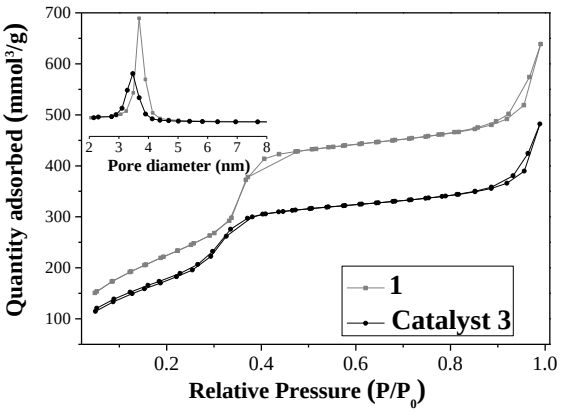

Figure 3. Nitrogen adsorption-desorption isotherms of **1** and catalyst **3**.

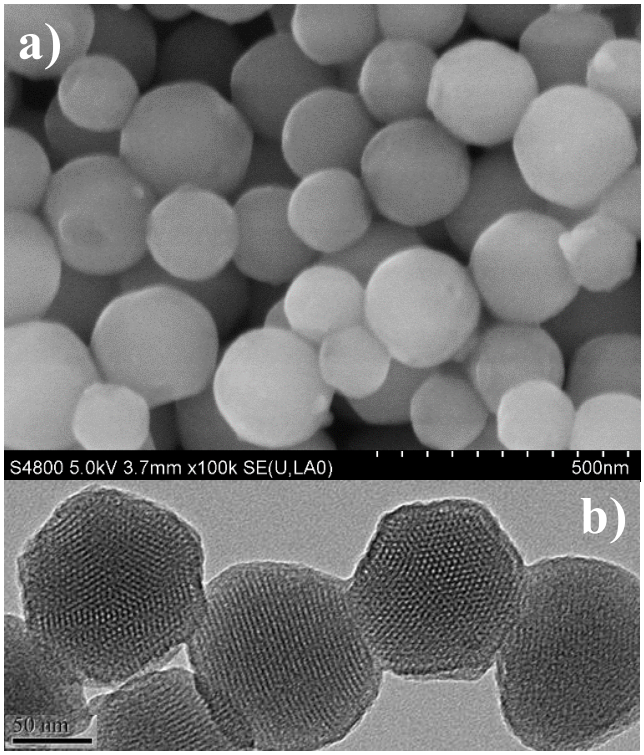

Figure 4. (a) SEM images of catalyst **3**, (b) TEM images of catalyst **3**.

Investigation of the factors affecting catalytic performance in the single-step asymmetric transfer hydrogenation

Chiral N-sulfonylated diamine-based organorhodium complexes and their cationic complexes as a type of efficient ATH catalysts are well-documented in the asymmetric transfer hydrogenation of α–haloketones.[5] In the present study, we first investigated the catalytic and enantioselective performance of catalyst **3** in the ATH of 2-bromophenylethanone in water. Due to a typical two-phase reaction system, this ATH reaction in water often needs cetyltrimethylammonium bromide acting as phase-transfe catalyst to promote its catalytic performance in a homogeneou catalysis.[5a] Because the designed heterogeneous catalyst **3** wa assembled through using cetyltrimethylammonium bromide as structure-directing template, the residual cetyltrimethylammoniur bromide in catalyst **3** is inevitable,[13] which could work as potential phase-transfer function to enhance its catalyti performance. Thus, in this case, the ATH of 2 bromophenylethanone catalyzed by **3** was carried out in th absence of cetyltrimethylammonium bromide, where the reactio was performed through the use of the HCO_2Na as a hydroge source and 1.0% mol **3** as a catalyst in water according to th reported method.[5a] It was found that the ATH of 2 bromophenylethanone catalyzed by **3** within 1 hour gave the (*R*) 2-bromophenylethanol in a quantitative yield with 99% *ee*. Such yield was comparable to that attained with its homogenou counterpart of $(Cp^*RhTsDPEN)^+BF_4^-$ (**2**) in the presence c cetyltrimethylammonium bromide as phase-transfer catalyst, an markedly better than that (86% yield) in the absence c cetyltrimethylammonium bromide reaction system, confirming th benefit of the designed catalyst **3.** Moreover, excelle enantioselective performance was similar to its homogenou counterpart of $(Cp^*RhTsDPEN)^+BF_4^-$ (**2**), suggesting that th $(Cp^*RhTsDPEN)^+BF_4^-$ active species in catalyst **3** keep it original homogeneous catalytic environment. This behavior coul be confirmed by a XPS investigation. As shown in Figure 5, it wa found that catalyst **3** had the similar Rh $3d^{5/2}$ electron bindin energy as the $(Cp^*RhTsDPEN)^+BF_4^-$ (309.10 eV versus 309.2 eV), demonstrating its catalytic environment did not chang during the immobilization process.

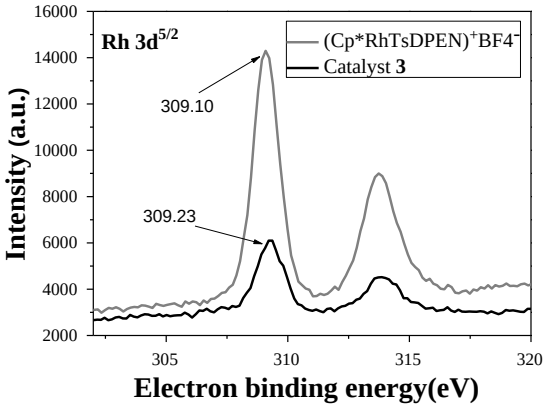

Figure 5. XPS spectra of the homogeneous $(Cp^*RhTsDPEN)^+BF_4^-$ (**2**) and catalyst **3**.

10.1002/cctc.201700436

In order to confirm its catalytic nature of catalyst **3** and to compare with its neutral counterpart, one kinetic investigation in the ATH of 2-bromophenylethanone catalyzed by catalyst **3,** its homogeneous $(Cp^*RhTsDPEN)^+BF_4^-$ and its neutral Cp*RhTsDPEN were performed. As shown in Figure 6, it was found that both catalyst **3** and its homogeneous $(Cp^*RhTsDPEN)^+BF_4^-$ had a higher initial activity than its neutral Cp*RhTsDPEN, where the initial TOFs for the ATH of 2-bromophenylethanone in 10 minute were 360 and 330 versus 252 $molmol^{-1}$ h^{-1}. This finding suggested that the cationic rhodium complex as active species could lead to a highly catalytic performance relative to that of the neutral Cp*RhTsDPEN, which is due to the lower energy barrier of cationic rhodium complex in the formation of Rh(III) formate intermediate confirmed by the proposed mechanism in the literatures.[11a, 14] This observation confirmed the catalytic nature of catalyst **3** and demonstrated the benefit of the designed heterogeneous catalyst.

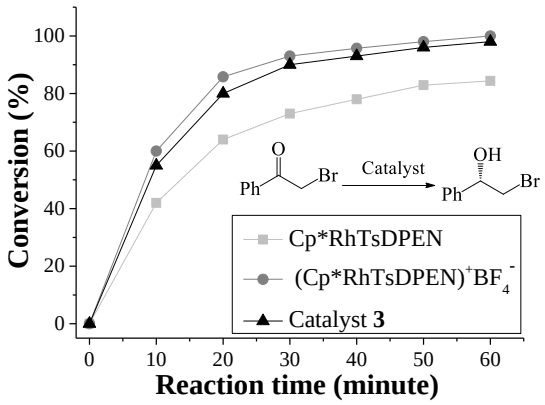

Figure 6. The ATH of 2-bromophenylethanone catalysed by catalyst **3**, its homogeneous $(Cp^*RhTsDPEN)^+BF_4^-$ and its neutral Cp*RhTsDPEN (Reactions were carried out at 25 °C, using 1.0 mol% of catalyst and 10 equiv. of HCOONa in 4.0 mL of water.

Catalytic properties of heterogeneous catalyst 3

On the basis of the obtained efficient asymmetric transfer hydrogenation, we then combined the ATH of 2-bromophenylethanone and the epoxidation of (*R*)-2-bromophenylethanol into the one-pot sequential organic transformation in water. It was found that this ATH/epoxidation enantio-relay reaction catalyzed by **3** could still afford the targeting products of (*R*)-2-phenyloxirane with 95% yield and 99% *ee* (Entry 1, Table 1). It was noteworthy that this result was markedly better than that obtained with the homogeneous mixed DABCO and $(Cp^*RhTsDPEN)^+BF_4^-$ as dual catalysts, since the latter only afforded the tiny targeting product due to the salinization of DABCO and 2-bromophenylethanone that was difficult to be epoxidated. This observation demonstrated the superority of the designed catalyst **3**, where the potentical site-isolated feature of bifunctionality in heterogeneous catalyst **3** could perform an efficient sequential organic transformation.

Having established the ATH/epoxidation enantio-relay reaction of 2-bromophenylethanone, catalyst **3** was further examined in the ATH/epoxidation enantio-relay reactions with a series of substituted substrates for investigation of its general applicability. As shown in Table 1, various 2–bromoketones could be steadily converted into the corresponding chiral products with high yields and enantioselectivities under the same reaction conditions. Also, it was found that the structures and electronic properties of the substituents at the aromatic ring group did not significantly affect their enantioselectivities regardless of the reactions with *para*- or *meta*- or *ortho*-position bromoacetophenone (Entries 2–10). Futhermore, besides organic transfromations of 2-bromoketones, 2-chloroketones could also be converted smoothly in this ATH/epoxidation catalysis sequence (Entries 11–14).

Table 1. The ATH/epoxidation enantio-relay reaction of 2-haloketone.[a]

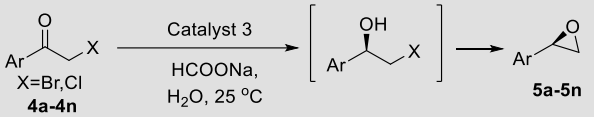

Entry	5	Ar	X	Yield (%)	Ee (%)[b]
1	**5a**	Ph	Br	95	99
2	**5b**	4-FPh	Br	93	96
3	**5c**	4-ClPh	Br	96	95
4	**5d**	3-ClPh	Br	92	95
5	**5e**	4-BrPh	Br	95	95
6	**5f**	3-BrPh	Br	93	95
7	**5g**	4-NO_2Ph	Br	90	82
8	**5h**	4-MePh	Br	96	93
9	**5i**	2-OMePh	Br	91	92
10	**5j**	2-naphthy	Br	97	96
11	**5k**	Ph	Cl	95	96
12	**5l**	4-FPh	Cl	92	94
13	**5m**	4-ClPh	Cl	95	92
14	**5n**	3-ClPh	Cl	93	95

[a] Reaction conditions: catalyst **3** (10.05 mg, 2.0 μmol of Rh, based on I analysis), HCO_2Na (137.0 mg, 2.0 mmol), 2-haloketone (0.20 mmol), and mL of water, reaction temperature (25 °C), reaction time (16-20 h)
[b] Determined by chiral HPLC analysis (see SI in Figures S5, S8).

Catalyst's stability and recyclability

As we designed another consideration in the construction of th heterogeneous catalyst **3**, it is to expect that the heterogeneou catalyst **3** could be easily recovered by simple centrifugation an the recycled catalyst **3** could keep its catalytic activity an enantioselectivity after multiple cycles. As observed, th heterogeneous catalyst **3** could be recovered easily through centrifugation and reused repeatedly in the ATH/epoxidation enantio-relay reaction of 2-bromophenylethanone. As shown in Table 2, in seven consecutive reactions, the recycled catalyst **3** still afforded (*R*)-2-phenyloxirane with 93% conversion and 95% *ee* (see SI in Figure S7). The obviously decreased reactivity at eighth recycle are attributed to the high Rh-leaching during the recycling. An inductively coupled plasma (ICP) optical emission spectrometer analysis disclosed that the amounts of Rh in catalyst **3** after eighth recycle was 17.86 milligrams per gram of catalyst, meaning 13.0 % of Rh loss. This value was obviously

10.1002/cctc.201700436

higher than that of the Rh-leaching after seventh recycle (19.06 milligrams per gram of catalyst and 7.1 % of Rh loss), indicating the high Rh-leaching at eighth recycle responsible for its low catalytic performance.

Table 2. Reusability of catalyst **3** for the ATH/epoxidation enantio-relay reaction of 2-bromophenylethanone.[a,b]

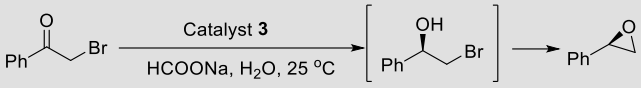

Run time	1	2	3	4	5	6	7	8
% conversion	99	99	98	98	99	95	93	82
% *ee*	99	99	97	97	97	96	95	95

[a] Reaction conditions: Catalyst **3** (100.50 mg, 20.0 μmol of Rh, based on ICP analysis), HCO_2Na (1.37 g, 2.0 mmol), 2-haloketone (2.0 mmol), and 30.0 mL H_2O, reaction temperature (25 °C), reaction time (16). [b] Determined by chiral HPLC analysis.

Expansion of one-pot enantio-relay reaction

In addition to the ATH/epoxidation one-pot enantio-relay reactions of aromatic 2-haloketone shown in Table 1, the heterogeneous catalyst **3** could also be applied to the synthesis of chiral β-amino alcohols through an amination/ATH enantio-relay sequence.[15] As shown in Table 3 this amination/ATH enantio-relay reactions catalysed by **3** could afford various β-amino alcohols in high yields and enatioselectivities. Taking the amination/ATH enantio-relay reaction of 2-bromophenylethanone and aniline as an example, the reaction catalyzed by **3** gave (*R*)-1-phenyl-2-(phenylamino)ethan-1-ol in 97% yield with 95% *ee*. As expected, the DABCO as a base in the heterogeneous catalyst **3** could promote the first-step amination whereas chiral cationic rhodium/diamine active species enabled an efficiently reduction process, further confirming the bifunctional benefit of the heterogeneous catalyst **3**.

Table 3. One-pot Synthesis of Chiral β-Amino Alcohols.[a]

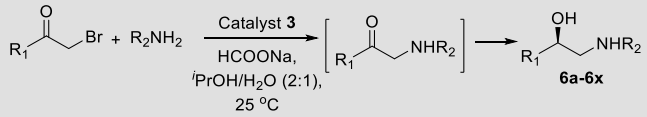

Entry	6	R_1	R_2	Yield (%)	Ee (%)[b]
1	**6a**	Ph	Ph	97	95
2	**6b**	4-FPh	Ph	98	95
3	**6c**	3-FPh	Ph	97	95
4	**6d**	4-ClPh	Ph	98	94
5	**6e**	3-BrPh	Ph	97	95
6	**6f**	4-NO_2Ph	Ph	94	89
7	**6g**	2-naphthyl	Ph	97	96
8	**6h**	Ph	4-ClPh	95	97
9	**6i**	Ph	3-ClPh	96	99
10	**6j**	Ph	3-NO_2Ph	95	97

[a] Reaction conditions: catalyst **3** (10.05 mg, 2.0 μmol of Rh, based on ICP analysis), HCO_2Na (137.0 mg, 2.0 mmol), 2-bromoketone (0.20 mmol), amine (0.24 mmol), and 3.0 mL of the mixed solvents (^{i}PrOH/H_2O, v/v = 2/1), reaction temperature (25 °C), reaction time (3-5 h).
[b] Determined by chiral HPLC analysis (see SI in Figures S6, S8).

Conclusion

In conclusions, by utilizing a hydrogen bonding strategy, w anchor conviently chiral cationic rhodium/diamine within base functionalized mesostructured silica nanoparticles, developing bifunctional catalyst. As demonstrated in the present study bifuctionality of base role and chiral cationic rhodium/diamin catalytic nature could perform cooperatively two kinds of enantic relay reactions, leading to the corresponding chiral products wit up to 99% enantioselectivity. This strategy described here nc only leverages the benefits of both homogeneous an heterogeneous catalysis to retain its catalytic performance, bu also exploits its sequential application of chiral 2–haloethanols Moreover, catalyst could be recovered and reused, showin particularly attractive in a two-step enantioselective organi transformation.

Experimental Section

Preparation of catalyst 3

In a typical synthesis, (*The first step for the synthesis of **1**)* 0.25 (0.17 mmol) of cetyltrimethylammonium bromide (CTAB) was adde to an aqueous solution (120 mL) of NaOH (0.88 mL, 2.0 M) at 70 °C After dissolution of CTAB, 1.40 g of TEOS (1.50 mL, 6.72 mmol) wa added and the mixture was stirred for 5~10 min. After that, 0.14 (0.38 mmol) of DABCO-derived siloxane was added to the system b dropwise, the mixture was stirred for another 5~10 min. Finally, th mixture was stirred vigorously for two hours at 80 °C. After cooling t room temperature, the solids were collected by centrifugation an washed repeatedly with excess distilled water. The surfactar template was removed by refluxing in a solution (80.0 mg c ammonium nitrate in 120 mL of ethanol) at 60 °C for 12 h. The solid was filtered and washed with excess water and ethanol, and dried a ambient temperature under vacuum overnight to afford DABCO@MSNs (**1**) as a white powder (0.83 g). (*The second step for the synthesis of **3***) The collected solids (0.50 g) was suspended in 20.0 mL of dry CH_2Cl_2, 34.50 mg (0.050 mmol) of $(Cp^*RhTsDPEN)^+BF_4^-$ (**2**) was added at room temperature and the resulting mixture was stirred at 25 °C for 12 h. The mixture was filtered through filter paper and then rinsed with excess CH_2Cl_2. After Soxhlet extraction for 4 h in CH_2Cl_2 to remove unreacted starting materials, the solid was dried at ambient temperature under vacuum overnight to afford DABCO@$(Cp^*RhTsDPEN)^+BF_4^-$@MSNs (**3**) (0.51 g) light−yellow powder. ICP analysis showed that the Rh loadings

were 20.52 mg (0.199 mmol) per gram of catalyst. ^{13}C CP/MAS NMR (161.9 MHz): 147.4−120.8 (C of Ph and Ar groups), 95.7 (C of Cp ring), 71.3−64.0 (C of –NCHPh), 62.1−56.1 (C of $–N^+CH_2–$ in CTAB molecule and C of $–N^+CH_2–$ in DABCO moiety), 53.3, 44.7 (C of $N(CH_2)_3–$ in DABCO moiety), 36.3−20.8 (C of $–CH_2Ph$, C of $–CH_2–$ in CTAB molecule and in DABCO moiety), 20.0−14.5 (C of $CH_3–$ in CTAB molecule and C of $–CH_2Si$), 9.0 (C of $–CH_3$ in $Cp(CH_3)_5$) ppm. ^{19}F MAS NMR (169.3 MHz): −166.0 ("bulk" BF_4^- species), −156~ −142 ppm (F in BF_4^- hydrogen bonded to the surface silanol group), −144.8 ("bulk" BF_4^- species), −123.6 (free BF_4^- species), −102.4 ("bulk" BF_4^- species), and −81.0 ("bulk" BF_4^- species) ppm. ^{29}Si MAS NMR (79.4 MHz): T^2 (δ = −60.1 ppm), T^3 (δ = −73.4 ppm), Q^2 (δ = −95.6 ppm), Q^3 (δ = −105.1 ppm), Q^4 (δ = −114.3 ppm).

General procedure for the ATH/epoxidation enantio-relay reaction of 2-haloketone

A typical procedure was as follows: Catalyst **3** (10.05 mg, 2.0 μmol of Rh, based on ICP analysis), HCO_2Na (137.0 mg, 2.0 mmol), 2-haloketone (0.20 mmol), and 3.0 mL H_2O, reaction temperature (25 °C), reaction time (16-20 h). During this period, the reaction was monitored constantly by TLC. After completion of the reaction, the catalyst was separated by centrifugation (10,000 rpm) for the recycling experiment. The aqueous solution was extracted with ethyl ether (3 × 3.0 mL). The combined ethyl ether extracts were washed with brine twice and then dehydrated with Na_2SO_4. After evaporation of ethyl ether, the residue was purified by silica gel flash column chromatography to afford the desired products. The *ee* values were determined by a HPLC analysis using a UV-Vis detector and Daicel chiralcel columns (Φ 0.46 × 25 cm).

General procedure for one-pot synthesis of chiral β-amino alcohols

A typical procedure was as follows. Catalyst **3** (10.05 mg, 2.0 μmol of Rh, based on ICP analysis), HCO_2Na (137.0 mg, 2.0 mmol), 2-bromoketone (0.20 mmol), amine (0.24 mmol), and 3.0 mL of the mixed solvents (^{i}PrOH/H_2O = 2:1), reaction temperature (25 °C), reaction time (3-5 h). During this period, the reaction was monitored constantly by TLC. After completion of the reaction, the catalyst was separated by centrifugation (10,000 rpm) for the recycling experiment. The aqueous solution was extracted with ethyl ether (3 × 3.0 mL). The combined ethyl ether extracts were washed with brine twice and then dehydrated with Na_2SO_4. After evaporation of ethyl ether, the residue was purified by silica gel flash column chromatography to afford the desired products. The *ee* values were determined by a HPLC analysis using a UV-Vis detector and Daicel chiralcel columns (Φ 0.46 × 25 cm).

Acknowledgements ((optional))

We are grateful to China National Natural Science Foundation (21672149), Ministry of Education of China (PCSIRT-IRT-16R49), Shanghai Sciences and Technologies Development Fund (13ZR1458700), the Shanghai Municipal Education Commission (14YZ074) for financial support.

Keywords: Asymmetric catalysis • Heterogeneous catalyst • Immobilization • Silica • Supported catalysts

[1] a) M. J. Climent, A. Corma, S. Iborra, *Chem. Rev.* **2010**, *111*, 1072-1133; b) M. J. Climent, A. Corma, S. Iborra, M. J. Sabater, *ACS Catal.* **2014**, *4*, 870–891; c) Y. M. He, Y. Feng, Q. H. Fan, *Acc. Chem. Res.* **2014**, *47*, 2894−2906; d) C. Li, H. D. Zhang, D. M. Jiang, Q. H. Yang, *Chem. Commun*. 2007, 547–558; e) Z. Wang, G. Chen, K. L. Ding, *Chem. Rev.* **2009**, *109*, 322–359; f) J. M. Fraile, J. I. García, J. A. Mayoral, *Chem. Rev.* **2009**, *109*, 360–417; g) M. Bartók, *Chem. Rev.* **2010**, *110*, 1663–1705; h) C. G. Yu, J. He, *Chem. Commun.* **2012**, *48*, 4933–4940; i) G. R. Cai, H. L. Jiang, *Angew. Chem. Int. Ed*. **2017**, 56, 563-567; j) X. Y. Yang, L. H. Chen, Y. Li, J. C. Rooke, C. Sanchez, B. L. Su, *Chem. Soc. Rev.* **2017**, 46, 481-558.

[2] a) J. M. Thomas, R. Raja, *Acc. Chem. Res.* **2008**, *41*, 708–720; b) D. E. De Vos, M. Dams, B. F. Sels, P. A. Jacobs, *Chem. Rev.* **2002**, *102*, 3615–3640; c) S. Minakata, M. Komatsu, *Chem. Rev.* **2009**, *109*, 711–724; d) M. Bartók, *Chem. Rev.* **2010**, *110*, 1663–1705; e) A. Mehdi, C. Reye, R. Corriu. *Chem. Soc. Rev.* **2011**, *40,* 563–574; f) H. Q. Yang, L. Zhang, L. Zhong, Q. H. Yang, C. Li, *Angew. Chem. Int. Ed.* **2007**, *4*(6861–6865.

[3] a) R. Srirambalaji, S. Hong, R. Natarajan, M. Yoon, R. Hota, Y. Kim, Y. Ko, K. Kim, *Chem. Commun.* **2012**, *48*, 11650–11652; b) K. C. Nicolaou D. J. Edmonds, P. G. Bulger, *Angew. Chem. Int. Ed.* **2006**, *45*, 7134 7186; c) N. R. Shiju, A. H. Alberts, S. Khalid, D. R. Brown, G Rothenberg, *Angew. Chem.* **2011**, *123*, 9789–9793; d) J. Y. Xu, T. Y Cheng, K. Zhang, Z. Y. Wang, G. H. Liu, *Chem. Commun.* **2016**, *52* 6005–6008.

[4] a) A. Fujii, S. Hashiguchi, N. Uematsu, T. Ikariya and R. Noyori, *J. Am Chem. Soc.* **1996**, *118*, 2521-2522; b) R. Malacea, R. Poli, E. Manoury *Coordin. Chem. Rev.* **2010**, *254*, 729–752; c) W. Yang, J.H. Xu, Y. Xie, Xu, G. Zhao, G. Q. Lin, *Tetrahedron: Asymmetry* **2006**, *17*, 1769-1774 d) S. Hashiguchi, A. Fujii, J. Takehara, T. Ikariya, R. Noyori, *J. Am Chem. Soc.* **1995**, *117*, 7562–7563; e) A. M. Hayes, D. J. Morris, G. Clarkson, M. Wills, *J. Am. Chem. Soc.* **2005**, *127*, 7318–7319; f) P. N Liu, P. M. Gu, F. Wang, Y. Q. Tu, *Org. Lett.* **2003**, *6*, 169–172; g) X. Wu X. Li, W. Hems, F. King, J. Xiao, *Org. Biomol. Chem.* **2004**, *2*, 1818 1821.

[5] a) F. Wang, H. Liu, L. Cun, J. Zhu, J. Deng, Y. Jiang. *J. Org. Chem.* **200** *70*, 9424-9429; b) J. Liu, D. Zhou, X. Jia, L. Huang, X. Li, A. S. C. Chan *Tetrahedron: Asymmetry* **2008**, *19*, 1824-1828; c) Y. Ma, H. Liu, L. Chen X, Cui, J. Zhu, J. Deng. *Org. Lett.* **2003**, *5*, 2103-2106; d) T. Ohkuma, H Tsutsumi, N. Utsumi, N. Arai, R. Noyori, K. Murata, *Org. Lett.* **2007**, 9 255-257; e) G. Xu, H. Yu, X. Zhang, J. Xu, *ACS Catal.* **2012**, *2*, 2566 2571; i) C. Lu, Z. Luo, L. Huang, X. Li, *Tetrahedron: Asymmetry* **2011**, *2* 722-727.

[6] a) Q. Q. Ye, T. Y. Cheng, Y. X. Zhao, J. W. Zhao, R. H. Jin, G. H. Liu *ChemCatChem* 2015, *7*, 1801-1805; b) J. Li, C. Wang, D. Xue, Y. Wei, Xiao, *Green Chem.* **2013**, *15*, 2685-2689; c) L. Li, S. B. Herzon, *J. Am Chem. Soc.* **2012**, *134*, 17376−17379; d) A. S. Rowan, T. S. Moody, P M. Howard, T. J. Underwood, I. R. Miskelly, Y. He, B. Wang *Tetrahedron: Asymmetry* **2013**, *24*, 1369-1381.

[7] a) J. W. Wiench, C. Michon, A. Ellern, P. Hazendonk, A. Iuga, R. Angelici, M. Pruski, *J. Am. Chem. Soc.* **2009**, *131*, 11801–11810; b) X. Z Shu, S. C. Nguyen, Y. He, F. Oba, Q. Zhang, C. Canlas, G. A. Somorja A. P. Alivisatos, F. D. Toste, *J. Am. Chem. Soc.* **2015**, *137*, 7083−7086 c) M. D. Jones, R. Raja, J. M. Thomas, B. F. G. Johnson, D. W. Lewis, Rouzaud, K. D. M. Harris, *Angew. Chem.* **2003**, *115*, 4462–4467; d) Y. L. Xu, T. Y. Cheng, J. Long, K. T. Liu, Q. Q. Qian, F. Gao, G. H. Liu, H. X. Li, *Adv. Synth. Catal*. **2012**, *354*, 3250–3258.

[8] a) T. Y. Cheng, Q. K. Zhao, D. C. Zhang, G. H. Liu, *Green Chem.* **2015**, *17*, 2100–2122; b) D. C. Zhang, X. S. Gao, T. Y. Cheng, G. H. Liu, *Sci. Rep.* **2014**, *4*, 5091–5097; c) D. C. Zhang, J. Y. Xu, Q. K. Zhao, T. Y. Cheng, G. H. Liu, *ChemCatChem* **2014**, *6*, 2998–3003; d) X. L. Xia, M. Wu, R. H. Jin, T. Y. Cheng, G. H. Liu, *Green Chem.* **2015**, *17*, 3916–3922; e) H. S. Zhang, R. H. Jin, H. Yao, S. Tang, J. L. Zhuang, G. H. Liu, H. X. Li. *Chem. Commun.* **2012**, *48*, 7874–7876.

[9] a) A. G. Ying, S. Liu, Y. X. Ni, F. L. Qiu, S. L. Xu, W. Y. Tang, *Catal. Sci.*

Technol. **2014**, *4*, 2115–2125; b) J. H. Li, W. J. Liu, Y. X. Xie, *J. Org. Chem.* **2005**, *70*, 5409–5412; (v) J. H. Li, W. J. Liu, *Org. Lett.* 2004, **6**, 2809–2811; d) L. R. Wen, M. C. Lan, W. K. Yuan, M. Li, *Org. Biomol. Chem.* **2014**, *12*, 4628–4632.

[10] a) M. Xue, J. I. Zink, *J. Phys. Chem. Lett.* **2014**, *5*, 839−842; b) K. Zhang, L. L. Xu, J. G. Jiang, N. Calin, K. F. Lam, S. J. Zhang, H. H. Wu, G. D. Wu, B. Albela, L. Bonneviot, P. Wu. *J. Am. Chem. Soc.* **2013**, *135*, 2427–2430; Z. A. Qiao, L. Zhang, M. Y. Guo, Y. L. Liu, Q. S. Huo, *Chem. Mater.* **2009**, *21*, 3823–3829; d) W. C. Yoo, A. Stein, *Chem. Mater.* 2011, **23**, 1761–1767; e) Z. Gao, I. Zharov, *Chem. Mater.* **2014**, *26*, 2030–2037; f) M. H. Wang, Z. K. Sun, Q. Yue, J. Yang, X. Q. Wang, Y. H. Deng, C. Z. Yu, D. Y. Zhao, *J. Am. Chem. Soc.* **2014**, *136*, 1884–1892; g) Y. Ma, L. Xing, H. Zheng, S. Che, *Langmuir* **2011**, *27*, 517–520; h) F. Q. Tang, L. L. Li, D. Chen, *Adv. Mater.* **2012**, *24*, 1504–1534.

[11] a) X. F. Wu, X. H. Li, A. Zanotti-Gerosa, A. Pettman, J. Liu, A. J. Mills, J. L. Xiao, *Chem. Eur. J.* **2008**, *14,* 2209–2222; b) X. F. Wu, J. Liu, D. D. Tommaso, J. A. Iggo, C. R. Catlow, J. Bacsa, J. L. Xiao, *Chem. Eur. J.* **2008**, *14,* 7699–7715; c) P. N. Liu, J. G. Deng, Y. Q. Tu, S. H. Wang, *Chem. Commun.* **2004**, 2070–2071; d) N. A. Cortez, G. Aguirre, M. Parra-Hake, R. Somanathan, *Tetrahedron:Lett.* **2009**, *50*, 2282–2291; e) T. Ikariya, A. J. Blacker, *Acc. Chem. Res.* **2007**, *40*, 1300–1308; f) J. E. D. Martins, G. J. Clarkson, M. Wills, *Org. Lett.* **2009**, *11***,** 847–850.

[12] J. Mao, D. C. Baker, *Org. Lett.* **1999**, *1*, 841–843.

[13] a) V. Cauda, A. Schlossbauer, J. Kecht, A. Zürner, T. Bein, *Am. Chem. Soc.* **2009**, *131*, 11361−11370; b) F. Gao, R. H. Jin, D. C. Zhang, Q. X. Liang, Q. Q. Ye, G. H. Liu, *Green Chem.* **2013**, *15*, 2208−2214.

[14] a) C. Pettinari, R. Pettinari, F. Marchetti, A. Macchioni, D. Zuccaccia, B. W. Skelton, A. H. White, *Inorg. Chem.* **200**7, *46*, 896–906. c) R. Noyori, M. Yamakawa, S, Hashiguchi, *J. Org. Chem.* **2001**, *66*, 7931–7944. d) M. Yamakawa, H. Ito, R. Noyori, *J. Am. Chem. Soc.* **2000**, *122*, 1466–1478.

[15] a) Q. Q. Ye, T. Y. Cheng, Y. X. Zhao, J. W. Zhao, R. H. Jin, G. H. Liu, *ChemCatChem* **2015**, *7*, 1801−1805; b) J. Li, C. Wang, D. Xue, Y. Wei, J. Xiao, *Green Chem.* **2013**, *15*, 2685−2689; c) L. Li, S. B. Herzon, *J. Am. Chem. Soc.* **2012**, *134*, 17376−17379.

Received: ((will be filled in by the editorial staff))
Published online: ((will be filled in by the editorial staff))

10.1002/cctc.201700436

FULL PAPER

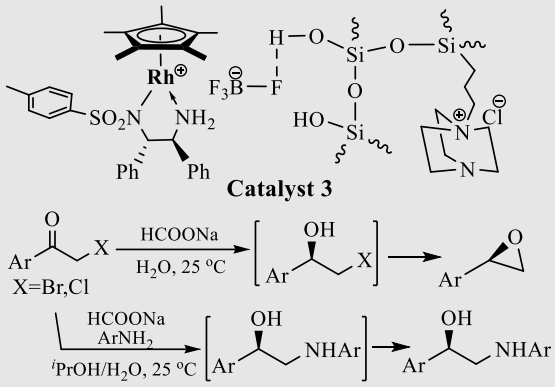

Assembly of cationic rhodium/diamine complex within base–functionalized mesostructured silica nanoparticles enables two kinds of efficiently enantioselective organinc transformations with high yields and enantioselectivities, where asymmetric transfer hydrogenation of α–haloketones followed by an epoxidation process provides various chiral aryloxirane while the amination of α–haloketones with anilines followed by asymmetric transfer hydrogenation produces various β-amino alcohols. Catalyst can be recovered and recycled for seven times without loss of its catalytic activity, showing an attracting feature in multi-step organic transformations in a sustainable benign process.

*Hang Liao, Yajie Chou, Yu Wang, Han Zhang, Tanyu Cheng and Guohua Liu**

Page No. – Page No.

Multi–Step Organic Transformations over Base–Rhodium/diamine–Bifunctionalized Mesostructured Silica Nanoparticles